Observation and Study of Land Surface Parameters over Gobi in Typical Arid Region[1]

Zhang Qiang (张 强), Cao Xiaoyan (曹晓彦) and Wei Guoan (卫国安)

Cold and Arid Regions Environment and Engineering Institute, Chinese Academy of Sciences, Lanzhou 730000

Huang Ronghui (黄荣辉)

Institute of Atmospheric Physics, Chinese Academy of Sciences, Beijing 100029

(Received November 27, 2000; revised July 23, 2001)

ABSTRACT

According to the need of popular land surface process models, characteristics and rules of some key land surface process and soil parameters over Gobi in typical arid region of Northwest China are analyzed by using the data observed during the intensive observation period of the Dunhuang Land-Surface Process Field Experiment (DLSPFE) (May–June 2000). Using the relative reflection as weighting factor, the weighted mean of the surface albedo over Dunhuang Gobi in typical arid region is calculated and its values are 0.255 ± 0.021. After canceling the interference of the buildings, the mean values of the roughness length averaged with logarithm is 0.0019 ± 0.00071 m. After removing the influence of the oasis, the soil wetness factor computed with data under condition of no precipitation is 0.0045. After removing the influence of the precipitation, the mean values of the soil heat capacity over Dunhuang Gobi in typical arid region is 1.12×10^6 J m^{-3}K^{-1}, a bit smaller than the values observed in HEIFE. But the soil heat diffusivity and conductivity are about one of those observed in HEIFE. The soil water content over Dunhuang Gobi in typical synoptic condition is very little and does not exceed 1% basically.

Key words: Gobi, Land surface parameters, Restraining factor to evaporation, Surface albedo, Roughness length, Soil heat diffusivity

1. Introduction

In U.S. Nation Report to International Union of Geodesy and Geophysics 1991–1994, Dickinson (1995) ever pointed out that improving land–surface process model which was coupled with the atmospheric model is one of two main aspects to raise the atmospheric model's simulation and predication ability. A few years ago the intercomparison of 25 international popular land–surface process models were made by Henderson–Sellers (1993) and it shows that the differences among these land–surface process models are very large. For example, the differences in mean values of the surface sensible and latent heat fluxes are as high as 17 W m^{-2}. The surface flux's uncertainty is very considerable to the atmospheric model. The physical parameter's difference between these models is the main reason that results of these models are different from each other (Zhang, 1998).

Desert and Gobi is the main land surface in arid region of Northwest China. They have

[1]This research was sponsored by the National Key Program for Developing Basic Sciences" Research on the Formation Mechanism and Prediction Theory of Heavy Climate and Synoptic Disasters in China" (No. G1998040904–2), the National Natural Science Foundation of China (No. 40175004) and Foreland Item of the Knowledge Innovation Field in Chinese Academy of Sciences (No. 210039).

special land surface physical process. It not only influences the global climate and the atmospheric circulation, but also has a strong action on the monsoon circulation in China and the arid climate in Northwest China. So, the accurate description of land–surface process over Desert and Gobi in arid region of Northwest China is becoming more and more important. Meanwhile, the study of the land–surface process parameters in arid region of Northwest China will be helpful to understand the hydrological and energy cycles in this region and can serve to the West Region Development.

Because the observation in arid region of Northwest China is scarce, the recognition on physical rule of land–surface process is limited and most of the land–surface parameters is uncertain, and even is unknown. Although HEIFE (Gao, 1992) and some other experiments promoted the understanding and recognition on land–surface process in arid region of Northwest China (Hu et al., 1992; Wang and Mitsuta, 1991; Hu et al., 1994; Zhang and Zhao, 1999), only a part of land–surface parameters were got and most of them are very rough. Up to now, there are still three main problems on land–surface process in arid region of Northwest China. The first is the influence of the oasis and the building on observation is not removed, because the influence of the oasis is strong since almost all of the observation stations are in or nearby the oasis. The second is the method to compute the parameters is unitary and the data to determine the parameters is not unified. The third is change of these parameters with solar altitude angle, soil wetness, cloud form and cloudiness is not deeply researched. Besides, the previous experiments were carried out in those arid areas where mean of annual precipitation is about 150 mm. But, in more arid climatic region where the mean of annual precipitation is even below 50 mm, such as Dunhuang, the land surface parameters in these regions should be different from those got in the previous experiments.

"Field Experiment on Interaction between Land and Atmosphere over Arid Region in Northwestern China" is one of two main field experiments of "Research on the Formation Mechanism and Prediction Theory of Heavy Climatic Disaster in China" which is one of the National Key Programs for Developing Basic Sciences. An intensive observation experiment was carried in Dunhuang observation station from May 25 to June 17, 2000 (briefly saying, "Dunhuang experiment"). A micrometeorological central station was set up in Gobi near Dunhuang oasis, a PAM station in Dunhuang Meteorological Station where in the oasis and an automatic meteorological station (AMS) in the transition area between oasis and Gobi. In this paper, the land surface process parameters are determined utilizing the "Dunhuang Experiment" data.

2. Observation field and instrumental precision

All data used in this paper were observed in Dunhuang Gobi micrometeorological central station from May 25 to June 17, 2000. The station is located at 40°10′N and 94°31′E, its surface elevation is 1150 meters above sea level and its annual mean of pressure is 873 hPa. The field is flat (the upper soil is mainly pebble, but the bottom is sand). The detailed description about the field refers to Zhang et al. (2001).

In "Dunhuang Experiment", a series of observations were conducted in Dunhuang Gobi micrometeorological central station, such as the gradients of wind, temperature and humidity, the components of radiation at surface, the temperatures near surface and in soil, the air humidity and heat fluxes in soil, and the fluctuations of wind, temperature and humidity of atmosphere. The soil water contents of two locations in Gobi were measured by using the weight method on June 16 (7:00–8:00 local time). The soil samples were extracted at 5 cm, 10

cm, 20 cm, 40 cm, 80 cm and 160 cm beneath the surface). Setting of these instruments was described in Zhang et al. (2001). The precision of the instrument is mostly same as what described in Zhang and Hu (1992) and Wang et al. (1992).

3. Observational analysis of land-surface parameters over desert and gobi in typical arid region

During "Dunhuang experiment", there are valid 445 sets of data which are hourly averaged and 10-day's data to show full diurnal variations. So the amount of samples of hourly data is 445 and that of diurnal variations is 10. Among the 10 days, one day is affected evidently by the precipitation, 5 days are overcast or cloudy, and four days are clear. The time described here is the local time in Dunhuang, which is later 1 hour and 42 minutes than Beijing Time.

3.1 *Land surface albedo*

The land surface albedo α is calculated from the observed radiation component

$$\alpha = R / Q \ , \tag{1}$$

where R is the surface reflected radiation, Q the total solar radiation received by the soil surface. Figure 1 shows the characteristics of diurnal variation of the surface albedo (a) and its mean (or fitted curve) (b) over Dunhuang Gobi. It is known that the albedo is varied between 0.15 and 0.45, and fluctuated up and down 0.25 except the morning and evening. The diurnal variation of mean abeldo over dry soil surface and the fitted curve of its variation are a bit larger in the morning and evening than in the noon. And the abeldo of dry soil surface is much lager than that of wet surface just after precipitation. It is shown that the variations of albedo are attributed to the solar altitude angle and the soil moisture. Since the soil wetness is not observed in the experiment, the fitted relation between the albedo and the solar altitude angle has to be derived by using the data not be influenced by precipitation. It is

$$\alpha = 0.25 + 0.00074 \times (12 - t_{\text{local}})^2 \ . \tag{2}$$

where t_{local} is the Dunhuang local time which substitutes for the solar altitude angle.

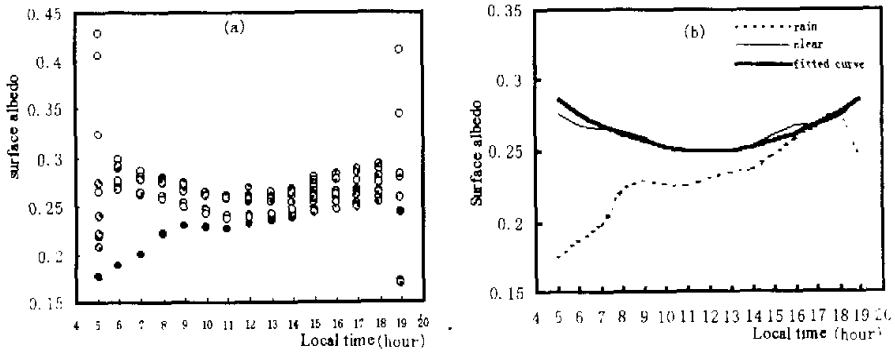

Fig. 1 Diurnal variation of surface albedo (a) and its mean or fitted curves (b) over Gobi (black dots are on rain days, grey dots are on cloudy days, blank circles are on clear days).

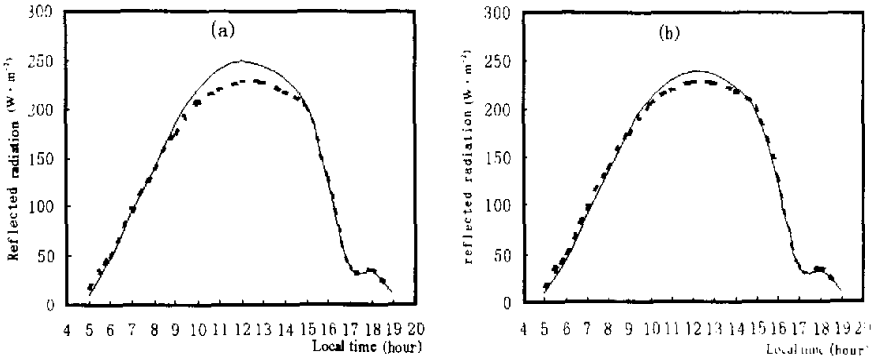

Fig. 2. Comparison of the diurnal variations of reflected radiation calculated by mean surface albedo (a) and weighted mean surface albedo (b) with observed values (solid curves express the observed values, dashed curves express calculated values).

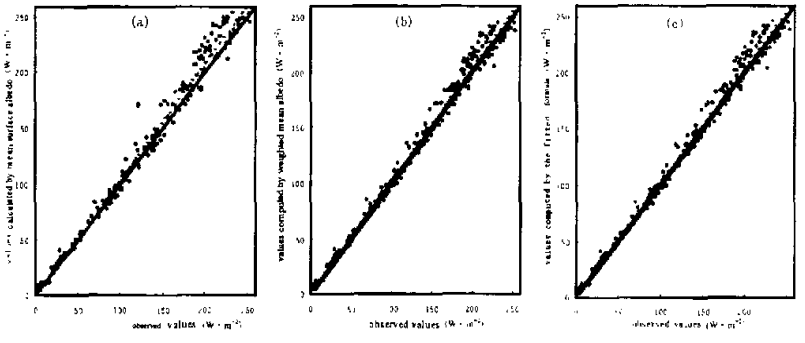

Fig. 3. Comparison of the reflected radiation computed by the mean albedo (a), the weighted mean albedo (b) and the fitted formula (2) (c) with the observed value.

The mean albedo not influenced by precipitation is 0.265 ± 0.020. But the surface reflected radiation calculated with such albedo is quite different from the real value at noon. As shown in Fig. 2a, typically, it may be as higher as 22 W m^{-2} than observed. The reason is that albedo is higher in both the morning and evening than normal and it must affect the mean albedo since the main contribution to mean reflected radiation comes from the reflected radiation near noon. So, it is suggested that the albedo may be calculated by using the weighted mean method

$$\bar{\alpha} = \sum_{i=1}^{n} \frac{R_i}{\sum_{i=1}^{n} R_i} \alpha_i \quad , \tag{3}$$

where the subscript i is time serial. The weighted mean albedo computed by the above formula is 0.255 ± 0.021. As shown in Fig. 2b, it is bigger only 11 W m^{-2} than that observed value at noon. And it is close to the desert surface albedo (0.250) given in Stull (1991). But it is

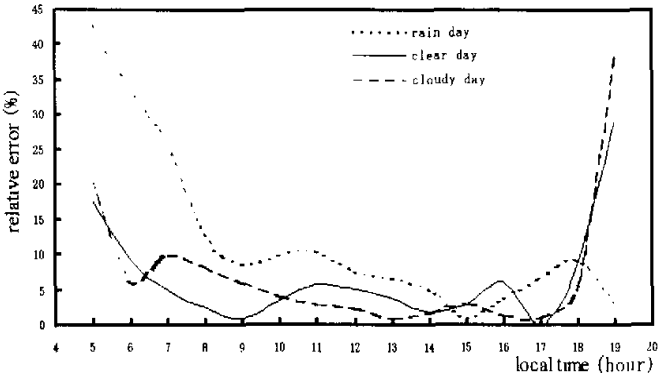

Fig. 4. Diurnal variation of the mean relative errors of the reflected radiations computed by the formula (2), in the clear days, cloudy days and the days just after rainfall.

obviously higher than those observed in HEIFE which are 0.228 over Gobi and 0.246 over desert (Zhou et al., 1992). Clearly, it is related to the climate in Dunhuang is drier than Heihe area.

Figure 3 shows that standard deviations of the reflected radiations, computed by the mean albedo, weighted mean albedo and that obtained by fitted formula, to the observed values are 6.37, 2.28 and 1.85 W m^{-2}, respectively, and their residuals are 0.89, −0.04 and −0.005 W m^{-2}, respectively. It is shown that the error of the reflected radiation computed by the mean albedo is the biggest. The error of the reflected radiation computed with the weighted mean albedo is close to that computed with the formula (2). Figure 4 shows the diurnal variation of the mean relative errors of the reflected radiation computed by the fitted formula (2), in the clear days, cloudy days and the days just after rainfall. It is shown that the relative errors are smaller in the clear and cloudy days than just after rainfall. Especially in the typical clear days, the relative errors during the period from 7:00 to 18:00 (the main period of contribution of the reflected radiation) is less than 5 per cent.

3.2 *Surface roughness length*

Based on Monin–Obukhov similarity theory, the roughness length z_0 can be calculated with the following formula

$$z_0 = z \times e^{-\left(\frac{\kappa V}{u_*} + \psi_m\right)}, \tag{4}$$

where κ is Von Karman constant and equals 0.4, generally; z the height, V the horizontal wind speed, u_* the turbulent friction velocity, ψ_m the integration form of Monin–Obukhov similarity function φ_m. It is difficult to calculate the roughness length because of its sensitivity, its calculation is difficult. In order to get a more reliable roughness length, the eddy correlation method, aerodynamic method and combinatory method will be used, respectively, to calculate the friction velocity.

3.2.1 *Eddy correlation method*

This method is conducted to compute the surface friction velocity directly using the instantaneous fluctuation data observed by the supersonic instrument.

$$u_* = \left[\overline{(u'w')^2} + \overline{(v'w')^2} \right]^{1/4}, \tag{5}$$

where u', v' and w' are the fluctuation of longitudinal, latitudinal and vertical wind speed respectively.

3.2.2 *Aerodynamic method*

The friction velocity is computed indirectly using the gradients data of wind speed, temperature and humidity at more than two levels.

$$\frac{\kappa z}{u_*} \frac{\partial V}{\partial z} = \varphi_m, \tag{6}$$

where φ_m is the Monin–Obukhov similarity function of speed. From Dyer and Hicks (1970) and Hicks (1976), the formula can be written as

$$\varphi_m = \begin{cases} (1 - 16\zeta)^{-1/4} & \zeta \leqslant 0 \\ (1 + 5\zeta) & \zeta > 0 \end{cases}, \tag{7}$$

where ζ is Monin–Obukhov atmospheric stability parameter (equals to z / L, where L is Monin–Obukhov atmospheric stability length) and can be approximately estimated by Businger–Dyer formula (Businger, 1988) as follows:

$$\zeta = \begin{cases} 1.0Ri & Ri < 0 \\ Ri / (1 - 5Ri) & Ri \geqslant 0 \end{cases}, \tag{8}$$

where Ri is Richardson number.

$$Ri = \frac{g(z_1 z_2)^{1/2}(\theta_2 - \theta_1)}{T(V_2 - V_1)^2} \ln(z_2 / z_1) \tag{9}$$

where the subscripts 1 and 2 denote two different levels.

3.2.3 *Combinatory method*

The friction velocity is computed indirectly from the gradient data and the surface radiation component (Hu and Qi, 1991).

$$u_* = u_{*0}(F / \alpha)^{1/2} \tag{10}$$

where F is the stratification modified function, α the ratio of the stratification modified function of momentum flux to one of heat flux

$$\alpha = \begin{cases} F^{1/3} & \partial\theta / \partial z \leqslant 0 \\ 1.0 & \partial\theta / \partial z > 0 \end{cases} \tag{11}$$

$$F = (R_n - G - S) / (H_0 + \lambda E_0) \tag{12}$$

where R_n is the net surface radiation, G soil heat flux and S heat storage. They can be found from the observed data. u_{*0}, H_0 and λE_0 can be calculated by

$$u_{*0} = \kappa(z_i z_{i+1})^{1/2} \frac{\partial V}{\partial z} \quad , \tag{13}$$

$$H_0 = -\rho c_p \kappa^2 z_i z_{i+1} \frac{\partial V}{\partial z} \frac{\partial \theta}{\partial z} \quad , \tag{14}$$

$$\lambda E_0 = -\rho \lambda \kappa^2 z_i z_{i+1} \frac{\partial V}{\partial z} \frac{\partial q}{\partial z} \quad . \tag{15}$$

Theoretically, the roughness length computed by the eddy correlation method should be the most precise because the turbulent flux is directly observed. In order to look for what causes the error of roughness length, it is also computed by combination of the friction velocity coming from the eddy correlation method with the horizontal wind speed at observed on the micrometeorological tower, and those observed by the supersonic instrument respectively. The roughness length is also calculated by combination of the friction velocity coming from the aerodynamic method and the combinatory method, separately, with the horizontal speed at 2 m observed on the micrometeorological tower. Therefore, in fact, we can get the roughness length by four ways.

Because the roughness length is very sensitive, the impacts of observational error and the interference of the buildings nearby may cause high scatters for the computed roughness length. Especially, when the wind speed is small, the roughness lengths at individual moments can differ in 2–3 orders from mean value and may have ill effect upon the roughness mean. Consider of z_0 takes effect in the logarithmic form in atmospheric models, a logarithmic average method is used to calculate the mean roughness length, i.e.,

$$\overline{z_0} = e^{(\sum \ln z_{0i})/n} \quad , \tag{16}$$

where i is time series. The logarithmic averaged roughness lengths are smaller bout one order than the general averaged ones. By means of logarithmic average, the values got by the combination of the friction velocities computed, respectively, by the eddy correlation method, aerodynamic method and combinatory method with the horizontal wind speed observed on the tower are $7.59 \times 10^{-4} \pm 2.24 \times 10^{-4}$ m, $2.96 \times 10^{-4} \pm 0.80 \times 10^{-4}$ m and $6.44 \times 10^{-4} \pm 1.11 \times 10^{-4}$ m. The differences are obvious, but are in the same order. It reflects the inconsistencies among of three methods in the respect of computing the friction velocities. The roughness length got by combination of from the friction velocity computed by the eddy correlation method with the horizontal wind speed observed by the supersonic instrument is $6.31 \times 10^{-3} \pm 0.10 \times 10^{-3}$ m. It is one order bigger than the above three values. It reflects the inconsistencies between the horizontal wind speeds observed by the photoelectric cup anemometer and supersonic fluctuation instrument. Meanwhile, three mean values of roughness lengths are computed by the combination of the friction velocities got by the aerodynamic method with horizontal wind speeds observed at 4, 8 and 18 m on the tower are $2.98 \times 10^{-4} \pm 1.80 \times 10^{-4}$, $3.03 \times 10^{-4} \pm 1.89 \times 10^{-4}$ and $3.36 \times 10^{-4} \pm 2.11 \times 10^{-4}$ m, respectively. They are close to the value computed by the horizontal wind speed at 2 m. That means the height has a little effect on calculation of roughness length. Such roughness length, from 0.05 m to 0.0003 m, over desert or Gobi can found in Dickinson et al. (1986) and Pielke (1990). But in the view of theory, this value ($6.31 \times 10^{-3} \pm 0.102 \times 10^{-3}$ m) got by the combination of friction velocity computed by the eddy correlation method with the horizontal wind speed observed by the supersonic fluctuation instrument is more credible. And Stull (1991) also suggests that the roughness length

over desert or Gobi should be in about the order of 10^{-3} m. The roughness length over desert and Gobi in Heihe area given out in other studies (Zuo and Hu, 1992; Chen et al., 1993) are in the same order.

The study (Zhang et al., 2001) has shown that the building (the Dunhuang Second Water Factory) near the observation field strongly interferes with the observation. It is the buildings to causes that the mean roughness lengths computed by the supersonic data bigger very much than those calculated from the data observed in HEIFE. The interference of the buildings can be mainly removed after canceling those data of which the buildings is located in upstream of the observational station. Fig. 5 is the diurnal variation of the roughness length computed by the supersonic data during all the 10 days (a) and the 4 days without interference of the buildings (b). It is shown that the roughness lengths are about 2 orders much longer during the period from 8:00 pm to 10:00 am, when data are interfered by the buildings frequently, than other values outside the period. And after canceling the interference of the buildings, the diurnal variation of the roughness length is close to the constant 0.002 m.

The roughness length computed by the formula (4) depends, in some extent, on Monin–Obukhov similarity function φ_m. In order to get the roughness length, as precious as possible, only those data in neutral status ($-0.1 < \zeta < 0.1$) are used to calculate it. The logarithmic mean of the roughness length computed by those data in neutral status is 0.0019 $\pm$ 0.00071 m, it closes to the value (0.002 m) mentioned above. Obviously, φ_m has little effect on roughness length. The logarithmic averaged values of roughness length are also close to those observed in Desert and Gobi in HEIFE (Zuo et al., 1992; Chen et al., 1993), which are bigger than those observed in Gobi in HEIFE by 0.0002–0.0007 m and less than an half of the values observed in desert in HEIFE. The reason is that the observational field is not flat and the sand ridges are nearly everywhere.

3.3 *Influence factor of the soil surface evaporation*

In Dickinson's land–surface process model (Dickinson et al., 1986), the water vapor transfer from soil surface to air is calculated by

$$E = -\rho C_D f_g (q_a - q_s) V_a \ , \tag{17}$$

where C_D is the coefficient of momentum bulk transfer; f_g the soil wetness factor which is used to modify saturated specific humidity near the surface if it is larger than those of observed; ρ atmospheric density; q_a and q_s specific humidity in surface layer and on surface,

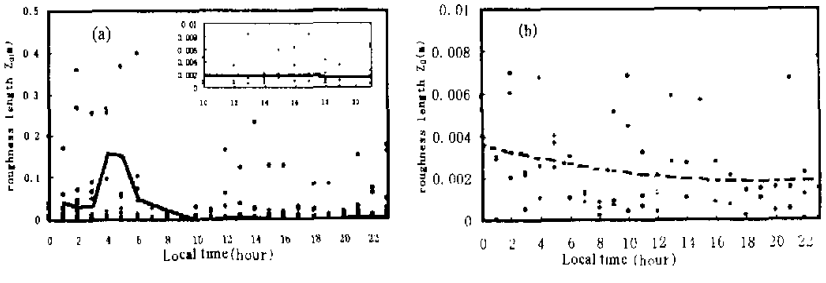

Fig. 5. The diurnal variation of the roughness length computed by the supersonic data during all the 10 days (a) and the 4 days without the interference of the buildings (b).

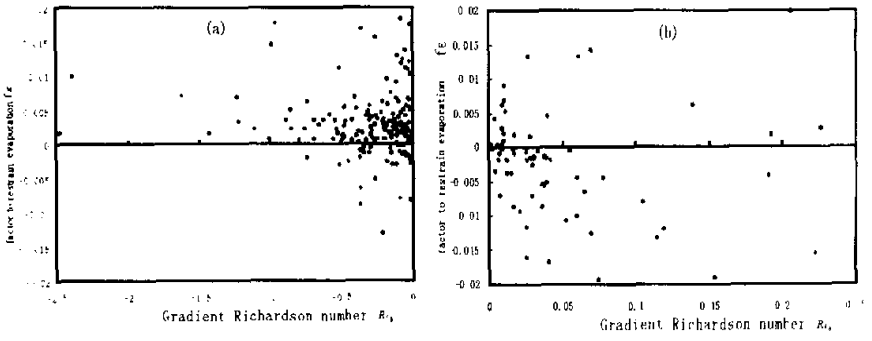

Fig. 6. The relationship of the restraining factor to restrain water vapor transfer f_E in unstable air (a) and in stable air (b) with Richardson number.

respectively; V_a horizontal wind speed in surface layer. It is assumed $C_D = C_q = C_H$ (C_H and C_q is the sensible and latent heat bulk transfer coefficients) in Formula (17). In fact, it is reasonable giving $C_q = C_H$. Since C_H can be got from the data, Formula (17) can be modified as

$$E = -\rho C_H f_g (q_a - q_s) V_a \quad . \tag{18}$$

For Gobi station in Dunhuang Experiment, the difference between the surface specific humidity and the surface saturation specific humidity is affected not only by the soil wetness, but also by the moisture advection from the west over Dunhuang oasis (Zhang et al., 2001). So Formula (18) can be modified as

$$E = -\rho C_H f_E (q_a - q_s) V_a = -\rho C_H (f_g + f_q)(q_a - q_s) V_a \quad . \tag{19}$$

where f_g is oasis moisture advection factor. f_g and f_q express the influence of the surface soil wetness and the moisture advection intensity on the difference between the surface specific humidity and the saturation specific humidity, respectively. And the soil moisture factor is always positive and the moisture advection factor is always negative. So, the restraining factor to water vapor transfer f_E can be defined as,

$$f_E = f_g + f_q \tag{20}$$

After canceling those data interfered by the buildings (in the wind direction from the buildings), the restraining factor to restrain water vapor transfer f_E can be got by the formula (19) using all remained data in other wind direction. As shown in Fig. 6, f_E prefers to positive in unstable air, and negative in stable air (i.e., negative gradient transfer). That means the moisture advection has big effect on f_E in stable air. This parameter can only describe the water vapor transfer characteristic over Desert and Gobi near oasis.

We can consider that the oasis moisture advection has no influence on the water vapor transfer, i.e., $f_q = 0$, if removing those data in which wind blew from the oasis (10°–180°) or atmospheric humidity is inverse. So, the soil wetness factor f_g can also be got from the formula (19). It is shown in Fig. 7 that soil wetness factor increases sharply and can enlarge almost to 1 because of increase of soil wetness just after rainfall (time series 1–12), after then it may decrease to and maintain 10^{-3} as long as the drying of surface soil. Also removing those

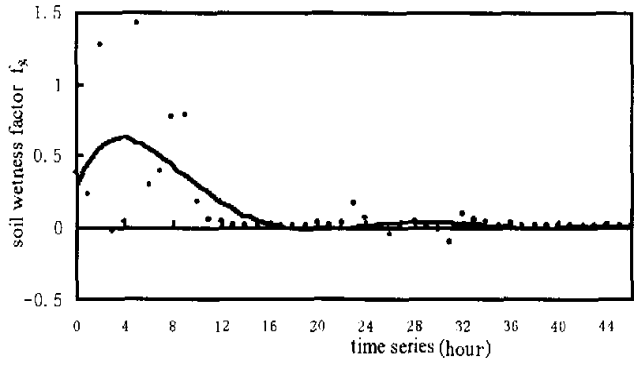

Fig. 7. Change of soil wetness factor along with time just after rainfall.

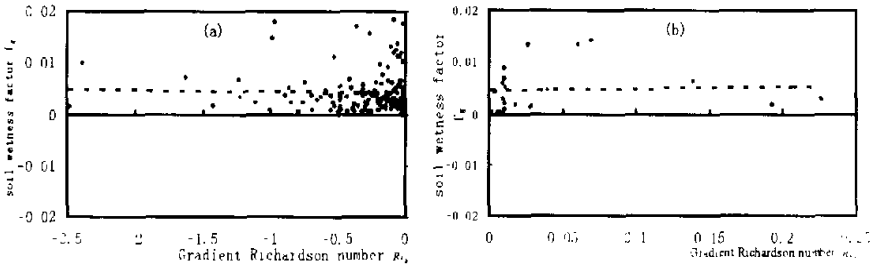

Fig. 8. The relationship of the soil wetness factor f_x in unstable air (a) and stable air (b) with Richardson number.

data affected by precipitation (188 observation time data remained), the soil wetness factor over typical Desert and Gobi can be calculated from the formula (19). As shown in Fig. 8, the soil wetness factor doesn't rely on Richardson number basically and the mean value is 0.0045 or so. The value can be used in the land–surface process model for arid regions.

The soil wetness factor is known as 0.0045, and it is easy to obtain the oasis moisture advection factor f_q from formula (19). Figure 9 shows the relationship of the oasis moisture advection factors f_q in unstable air (a) and stable air (b) with Richardson number. Obviously, the moisture advection factors are mainly negative. Contribution of moisture advection factor to f_E increases with the increase of stability, and vice versa. Its effect can be omitted if Richardson number is smaller than −1.2. The fitted formula of f_q against Richardson number is

$$f_q = \begin{cases} -0.004(1+2.5Ri_b) & Ri_b \geq 0 \\ -0.004(1+0.83Ri_b) & 0 < Ri_b \leq 1.2 \\ 0 & Ri_b > 1.2 \end{cases} \tag{21}$$

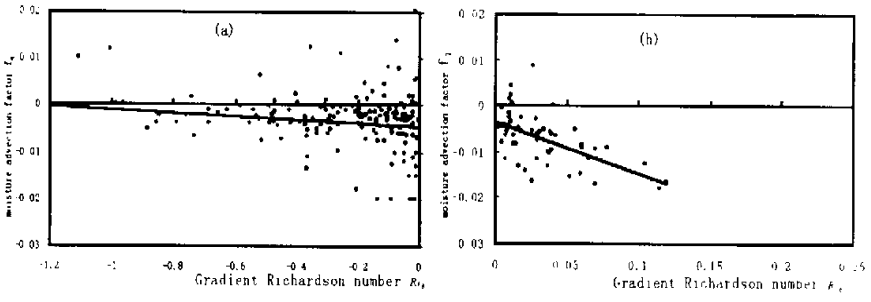

Fig. 9. Change of moisture advection factor with Richardson number in unstable (a) and stable air (b).

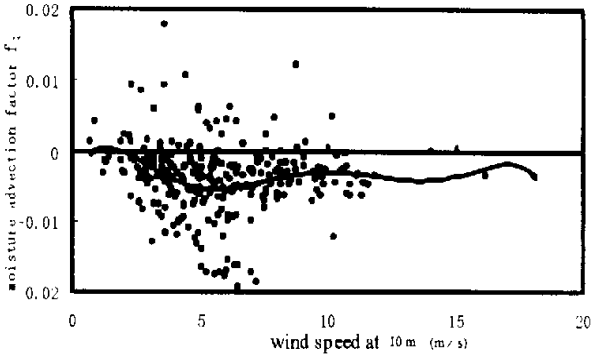

Fig. 10. The relationship of moisture advection factor over oasis with the horizontal wind speed.

It is shown formula (21) that f_q depends on Richardson number. This reason is that the turbulent mixing and its disintegration to moisture advection are getting stronger and the contribution of the moisture advectoin to f_q getting weaker as long as the air instability is getting stronger, and vice versa.

Figure 10 shows the relationship of moisture advection factor with the horizontal wind speed. Because the difference of air humidity between oasis and Gobi varies a little, the horizontal wind speed becomes the most important parameter to express the intensity of moisture advection over oasis. As shown in Fig. 10, the contribution of the moisture advection factor to f_E is getting larger along with the increasing of horizontal wind speed below 5 m s^{-1}, getting weaker along with the increasing of horizontal wind speed above 5 m s^{-1}, and getting no variation along with the increasing when horizontal wind speed above 10 m s^{-1}. The reason is that the horizontal wind speed to express not only intensity of moisture advection but also the intensity of wind speed shear, and the two effects are opposite each other.

4. Observational analysis of soil thermal transfer parameter

The soil thermal capacity C_s between 2.5 and 7.5 cm beneath the surface, and the soil thermal diffusivities K_s and the soil thermal conductivities λ_s at 2.5 and 7.5 cm beneath the surface can be calculated, respectively, using the data observed in this experiment by the following formulae:

$$C_s = (G_1 - G_2) / \left[\delta z (\partial T_g / \partial t) \right] , \tag{22}$$

$$\lambda_{si} = - G_i / (\partial T_g / \partial z) , \tag{23}$$

$$K_{si} = \lambda_{si} / C_s , \tag{24}$$

where G_1 and G_2 are the soil heat flux at 2.5 and 7.5 cm, respectively; δz the soil thickness of 5.0 cm between two levels at which heat flux is observed; $\partial T_g / \partial t$ the variability of soil temperature at 5.0 cm beneath the surface; the subscript i denotes level of 2.5 cm or 7.5 cm; and $\partial T_g / \partial z$ the temperature gradient between 0 and 5 cm, or 5 cm and 10 cm beneath the surface.

Table 1. The means of soil heat parameters at different level

	Thermal capacity (J m^{-3} K^{-1})	Thermal conductivity (W m^{-1} K^{-1})		Thermal diffusivity (m^2 s^{-1})	
	2.5 cm–7.5 cm	2.5 cm	7.5 cm	2.5 cm	7.5 cm
mean	$(1.12 \pm 0.27) \times 10^6$	0.177 ± 0.019	0.274 ± 0.017	$(1.65 \pm 0.49) \times 10$	$(2.52 \pm 0.63) \times 10$

As shown in Table 1, these means of soil parameters are reasonable, basically. The variations with the depth are clearly. The means of heat capacity of soil surface is a bit smaller than those observed in Gobi (in HEIFE, 1.23×10^6 J m^{-3} K^{-1}, Hu and Qi, 1991) in desert (1.28×10^6 J m^{-3} K^{-1}, Oke, 1978). Both the heat diffusivities at two levels are about an half of that observed in Gobi in HEIFE, but the value at 7.5 cm is close to that given in a representative paper desert (0.24×10^{-6} m^2 s^{-1}, Stull, 1991). Similarly, the means of heat conductivities are also smaller than that observed in HEIFE, but the value at 7.5 cm is close to that given in a paper (0.30 W m^{-2} K^{-1}, Oke, 1978). All mean values of the three soil heat parameters in this paper are smaller, in different extent, than those obtained in HEIFE. Maybe it is related to the soil in Duhuang is drier than in Heihe area. The parameters obtained in this paper are closer to those in representative papers.

The soil parameters are sensitive to the soil wetness. But it is regretted there is no soil wetness observation during the period of intensive observation period. In original research plan, we initiated to analyze, indirectly, the influence of the soil wetness by using rainfall data. The results are not satisfied. It is found, furtherly analyzing the data, that the influence of the rainfall on soil is reduced rapidly with depth and time because the rainfall during the intensive observation period is merely little (1 mm or so) while the evaporation force on Gobi surface is strong. The relative error is risen since small heat flux during rainfall.

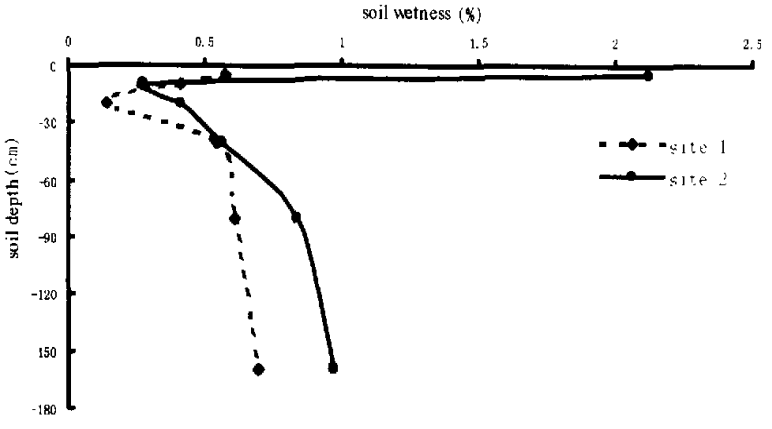

Fig. 11. The vertical profiles of the soil water content in soil at two points in Dunhuang Gobi, at 7:00–8:00 (local time), June 16, 2000 (a typical clear day).

5. Observational analysis for the vertical curve of water content in soil

The observation of the water content in soil in arid area is helpful to understand the rule of soil water transfer. Fig. 11 shows the vertical profiles of t water content in soil at two observation points in Dunhuagn Gobi at about 7:00–8:00 (local time), June 16, 2000 (a typical clear day). The water content in soil is very small and less than 1%. Its minimal value is not at the surface, as imaging as, but at the depth between 10 and 20 cm. The values have merely no variation with the depth, beneath the depth of about 60 cm. Such distribution of the soil moisture is probably related to soil absorption of sweat in air. It is just coincides tallies with so called " the soil respiration action" in desert or Gobi near oasis put forward early (Zhang and Zhao, 1999).

6. Conclusion and discussion

In the paper, using the relative reflected radiation as weighted factor, the mean albedo over Dunhuang Gobi is calculated as 0.255 ± 0.021. It is close to those given in representative papers and bigger than those observed in HEIFE. It reflects the influence of the climate in Dunhuang where is drier than Heihe area.

The roughness length is computed by the friction velocities obtained by the eddy correlation method, aerodynamic method and combinatory method, respectively. In order to remove the influence of abnormal roughness lengths on the mean value, we put forward a logarithmic mean method. It has positive effect even in the case of serious scattered roughness length. After canceling the interference of the buildings, the mean roughness length computed by the logarithmic mean method is 0.0019 ± 0.00071 m. It is close to that observed in HEIFE.

The restraining factor to water vapor transfer is calculated. It is key parameter to calculate the surface evaporation, especially, in arid areas. And the contributions of both factors of the soil wetness factor and moisture advection factor are derived, separately, in this paper. The soil wetness factor is 0.0045. And the relationships of the moisture advection factor with Richardson number and the horizontal wind speed are described, respectively.

The mean of soil heat capacity in typical arid area in Dunhuang Gobi is 1.12×10^6 J m^{-3} K^{-1}. It is a bit smaller than those observed in Gobi in HEIFE and in desert given by other studies. Both the soil heat conductivity and diffusivity at two levels are about half of those observed in Gobi in HEIFE, but close to those observed in desert given in some representative papers.

The soil water content is much small and does not exceed 1%. In the morning, its minimum is at the depth of about 10–20 cm, not at the soil surface. Finally, the variation of the land–surface process parameters, such as the surface albedo, with the soil wetness can't be derived because the soil wetness observations are absent during the IOP. It should be done in hereafter observations.

The authors would like to express our thanks to Hu Zeyong, Hou Xuhong, Nie Yanjiang and Yan Yuping for their helps.

REFERENCES

Businger, J. A., 1988: A note on the Businger–Dyer profiles. *Bound.-Layer Meteor.*, **42**, 145–151.

Chen Jiayi, Wang Jiemin, and Horiguchi Mitsuaki, 1993: An independent method to determine the surface roughness length. *Chinese J. Atmos. Sci.*, **17**(1), 21–26 (in Chinese).

Dickinson, R. E. et al., 1986: Biosphere–Atmosphere Transfer Scheme (BATS) for the NCAR Community Climate Model, NCAR / TN–275+STR, 12–51.

Dickinson, R. E., 1995: Land–atmosphere interaction, U. S. Nation Report to International Union of Geodesy and Geophysics 1991–1994, 917–922.

Dyer, A. J., and B. B. Hicks, 1970: Flux gradient transport of heat water in an unstable atmosphere. *Quart. J. Roy. Meteor. Soc.*, **93**, 501–508.

Gao Youxi, 1992: HEIFE Report No.1, Preface. *Plateau Meteorology*, **9**(2), (in Chinese).

Henderson-Sellers, A., 1993: The project for intercomparison of land–surface parameterization Schemes. *Bull. Amer. Meteor. Soc.*, **74**(7), 1335–1348.

Hicks, B. B., 1976: Wind profile relationships from the Wangara experiment. *Quart. J. Roy. Meteor. Soc.*, **102**, 535–551.

Hu Yinqiao, Qi Yeujin, and Yang Xuanli, 1990: Preliminary analysis about characteristics of microclimate and heat budget in Hexi Gobi (Huayin). *Plateau Meteorology*, **9**(2), 113–119 (in Chinese).

Hu Yinqiao, and Qi Yuejin, 1991: The combinatory method for determination of the turbulent fluxes and universal functions in the surface layer. *Acta Meteor. Sinica*, **49**(1), 46–53.

Hu Yinqiao, Yang Xuanli, and Zhang Qiang, 1992: The characters of energy budget on the Gobi and desert surface in Hexi Region. *Acta Meteor. Sinica*, **26** 82–91.

Hu Yinqiao, Gao Youxi, and Wang Jiemin, 1994: Some achievements in scientific research during HEIFE. *Plateau Meteor.*, **13**(3), 225–236 (in Chinese).

Oke, T. R., 1978: *Boundary Layer Climate*, London Methuen and COLTD, New York, 435.

Pielke, R. A., 1990. *Meso–scale Meteorological Simulation*, translated by Zhang Xinzhen and Yang Changxin, China Meteorological Press, Beijing, 677 (in Chinese).

Stull, R. B., 1991: *Introduction to Boundary Layer Meteorology*, translated by Yang Changxin, China Meteorological Press, Beijing, 401–405 (in Chinese).

Wang Jiemin, and Yasushi Mitsuta, 1991: Turbulence structure and transfer characteristics in the surface layer of the HEIFE Gobi area. *J. Meteor. Soc. Japan*, **69**(5), 587–593.

Wang Jiemin, Cui Tiemin, Yasushi Mitsuta, and Horiguchi Mitsuaki, 1992: A real–time, low cost turbulence data acquisition and processing system. *Plateau Meteor.*, **11**(4), 451–490 (in Chinese).

Zhang Qiang, 1998: Simple review of land surface process model. *Scientia Meteorologica Sinica*, **18**(3), 295–304 (in Chinese).

Zhang Qiang, and Zhao Ming, 1999: Field experiment and numerical simulation of inverse humidity of atmosphere

over desert near oasis. *Acta Meteorologica Sinica*, **57**(6), 729–740 (in Chinese).

Zhang Qiang, Wei Guoan, and Huang Ronghui, 2001: The study of the atmospheric bulk transfer coefficient over Desert and Gobi in arid region of northwestern China. *Science in China (Series D)*, **31**(9), 783–792 (in Chinese).

Zhang Qiang, and Hu Yinqiao, 1992: The instrumental accuracy and observational error about micrometeorological mast of Chinese side in "HEIFE". *Plateau Meteor.*, **11**(4), 460–469 (in Chinese).

Zhou Jiling, Hou Xuhong, and Ji Guoliang, 1992: Preliminary study of solar radiation properties in HEIFE area in late summer. *Plateau Meteor.*, **11**(4), 381–388 (in Chinese).

Zuo Hongchao, and Hu Yinqiao, 1992: The bulk transfer coefficient over Desert and Gobi in the Heihe region. *Plateau Meteorology*, **13**(3), 282–290 (in Chinese).

典型干旱区荒漠戈壁陆面参数的观测研究

张 强 曹晓彦 卫国安

摘 要

根据目前流行的陆面过程模式的需要，利用2000年5–6月敦煌陆面过程野外观测实验加强期的观测资料，分析了西北典型干旱区荒漠戈壁的一些关键陆面过程和土壤参数的特征和规律。并且利用相对反射为权重加权平均，计算得到典型干旱区敦煌荒漠戈壁的平均反射率为0.255±0.021；剔除建筑物干扰后，利用对数平均法计算的粗糙度长度平均值为0.0019±0.00071 m；剔除绿洲影响后，用无降水影响的资料确定出土壤湿度影响因子为0.0045；剔除降水影响后，用观测资料计算的敦煌典型干旱区荒漠戈壁的热容量平均值为1.12×10^{6} J m^{-3} K^{-1}，比"黑河试验"在戈壁和在其它沙漠观测的有关值略小一些，但热扩散率和热传导率都比"黑河试验"在戈壁观测的值小一倍左右；观测的敦煌戈壁典型天气条件下的土壤含水量非常小，基本上不超过1%。

关键词：戈壁，陆面参数，水汽输送约束因子，粗糙度长度，土壤热扩散率